ISSN 1067-8212, Russian Journal of Non-Ferrous Metals, 2017, Vol. 58, No. 2, pp. 109–113. © Allerton Press, Inc., 2017.
Original Russian Text © A.S. Yasinskiy, P.V. Polyakov, A.B. Klyuchantsev, 2017, published in Izvestiya Vysshikh Uchebnykh Zavedenii, Tsvetnaya Metallurgiya, 2017, No. 1, pp. 13–18.

METALLURGY
OF NONFERROUS METALS

Motion Dynamics of Anodic Gas in the Cryolite Melt–Alumina High-Temperature Slurry

A. S. Yasinskiy*, P. V. Polyakov, and A. B. Klyuchantsev*****

Siberian Federal University, Krasnoyarsk, 660025 Russia

**e-mail: ayasinskiykrsk@gmail.com*

***e-mail: p.v.polyakov@mail.com*

****e-mail: akeyev@gmail.com*

Received October 6, 2015; in final form, November 11, 2015; accepted for publication November 12, 2015

Abstract—The results of physical simulation of the behavior of bubbles formed due to the electrochemical evolution of oxygen on an inert anode during the high-temperature electrolysis of alumina slurry in the fluoride melt are presented. Similarity criteria are calculated, the experiments for a water model with vertically oriented electrodes are performed, and the data on the behavior of bubbles in the slurry are found with the help of video recording. The 20% aqueous solution of sulfuric acid with an alumina content of 30 vol % was used as the model electrolyte. The experiments were performed in a range of current densities from 0.05 to 0.25 A/cm^2. Video was recorded using a Nikon D3100 camera with a recording frequency of 30 frames/s. The data on the motion dynamics of the bubbles, the quantitative data that characterize coalescence, and the bubble lifting velocity are found. To determine the average lifting velocity, 125 bubbles were analyzed. They were 0.8–2.3 mm thick. The bubble motion is performed in the slug regime with lifting velocity of 1.0–2.3 cm/s. The bubble layer thickness was about 5 mm. Further investigations will be directed to finding new data on the behavior of bubbles for various solid phase contents, current density, electrode slope angle, and granulometric composition.

Keywords: dimensional analysis method, similarity criteria, high-temperature slurry electrolysis, non-Newtonian fluid dynamics, inert anodes, low-temperature electrolysis of cryolite–alumina melts, aluminum electrowinning

DOI: 10.3103/S1067821217020122

INTRODUCTION

Currently, the only method of industrial aluminum production is the Hall–Heroult method, according to which alumina is subjected to electrolytic dissociation in the cryolite melt at ~960°C between horizontally arranged electrodes with a potential difference of ~4.2 V. One topical problem of aluminum industry which is being solved by aluminium companies and institutions worldwide is the development of inert anodes.

Another developmental direction of the Hall–Heroult method is low-temperature electrolysis in molten salts with a low liquidus temperature (lower than 700°C; for example, KF–AlF_3). Currently, none of these developments has obtained industrial application. In order to subsequently develop the Hall–Heroult method, including the development of inert anodes and low-temperature electrolysis, fundamental investigations are required, among which the physical simulation method and similarity theory occupy a separate place.

The similarity theory is widely used to solve various problems of mechanics, fluid dynamics, and other sciences [1, 2]. Most problems requiring physical simulation include the calculation of similarity criteria. Our article is devoted to solving the gas dynamics problem of electrolytically formed oxygen bubbles when producing aluminum using a new method. It is based on low-temperature slurry electrolysis with the vertical arrangement of electrodes using inert anodes [3–5]. There is no published information on the bubble motion during electrolysis in conditions of the straitened motion confined by the electrode surface and slurry layer.

Aluminum electrowinning by low-temperature ($t \approx$ 700°C) electrolysis with a high content of undissolved alumina (>30 vol %) substantially limits the possibilities of the visual observation of accompanying phenomena. We simulated the motion of oxygen bubbles forming on the electrode surface due to the electrochemical alumina decomposition in the fluoride melt according to the reaction

$$2O^{2-}_{(k)} - 4e \rightarrow O_2, \quad (1)$$

Table 1. Similarity criteria

Criterion	Exponent at parameter								Remark
	ω	h	l	v	ν	g	σ	γ	
π_1	1	1	0	0	−1	0	0	0	Reynolds criterion
π_2	0	1	0	1	−1	0	0	0	Bukhbinder criterion
π_3	0	3	0	0	−2	1	0	0	Galilean criterion
π_4	0	1	0	0	−2	0	1	−1	Weber criterion
π_5	0	1	−1	0	0	0	0	0	Geometric simplex

where O^{2-} ion comprises the composition of the $O^{2-}_{(k)}$ oxyfluoride complex.

The character of the bubble motion determines key process parameters of electrolysis such as the anode–cathode distance, specific electricity consumption, and current efficiency. Target problem parameters, which characterize the bubble behavior, are the lifting velocity, the bubble growth rate, and the bubble layer thickness. It should be noted that the dynamics of the bubble motion is not the main question, but only a partial one in development of a new aluminum electrowinning method using inert anodes. The questions of corrosion of metallic anode in the slurry, anodic, and cathodic overvoltages and mass transfer during the electrolysis, as well as the electrical conductivity of slurries, are worth separate attention. These questions will be considered in subsequent publications.

PHYSICAL SIMULATION

The problem of simulating electrolytically formed bubbles in molten salts was solved by the authors of [6–13]. The investigation of the fluid dynamics phenomena occurring during the electrolysis was required using the low-temperature model. According to [8], the equation, which describes the gas motion in the liquid medium (without slurries), has the form

$$\omega = f(h, v, \nu, l, g, \gamma, \sigma), \tag{2}$$

where ω is the bubble motion velocity, m/s; h is the electrode height, m; l is the anode–cathode distance, m; v is the specific gas evolution rate, $m^3/(m^2\ s)$; ν is the kinematic viscosity, m^2/s; g is the acceleration of gravity, m/s^2; γ is the electrolyte density, kg/m^3; and σ is the electrolyte surface tension, J/m^2 (kg/s^2).

The motion mechanism of oxygen bubbles in the slurry will not differ from the motion mechanism of chlorine [8] and carbon dioxide [9]. Equation (2) will be also valid for the solved problem. Applying the method of analysis of dimensionalities and π theorem, we can transform expression (2) into the criterion equation, which consists of dimensionless complexes (similarity complexes) and simplexes.

Let us specify three main parameters: ν, γ, and h. Then the criterion equation will take the form

$$\frac{\omega}{\nu^{a_1}\gamma^{a_2}h^{a_3}} = f\left(\frac{v}{\nu^{b_1}\gamma^{b_2}h^{b_3}}, \frac{l}{\nu^{c_1}\gamma^{c_2}h^{c_3}}, \frac{g}{\nu^{d_1}\gamma^{d_2}h^{d_3}}, \frac{\sigma}{\nu^{e_1}\gamma^{e_2}h^{e_3}}\right). \tag{3}$$

To determine the first criterion, which is arranged in the left part of Eq. (3), we should find values of a_1, a_2, and a_3 in the expression

$$[L][T]^{-1} = ([L]^2[T]^{-1})^{a_1}([M][L]^{-3})^{a_2}[L]^{a_3}. \tag{4}$$

Solving the set of equations

$$\begin{cases} 2a_1 - 3a_2 + a_3 = 1, \\ a_2 = 0, \\ -a_1 = -1, \end{cases} \tag{5}$$

we will derive

$$\begin{cases} a_1 = 1, \\ a_2 = 0, \\ a_3 = -1. \end{cases} \tag{6}$$

Thus, first similarity criterion π_1 will have the form

$$\pi_1 = \omega h/\nu. \tag{7}$$

It is evident that the first criterion is the Reynolds criterion. Other criteria can be calculated in a similar manner. The results are presented in Table 1.

By the proposal of the authors of [8], criterion π_2 is called as the Bukhbinder criterion. It is also known in publications as the modified Reynolds criterion.

Thus, the criterion equation will have the form

$$\frac{\omega h}{\nu} = B\left(\frac{vh}{\nu\gamma}\right)^m\left(\frac{gh^3}{\nu^2}\right)^n\left(\frac{\sigma h}{\nu^2\gamma}\right)^q\left(\frac{h}{l}\right)^p. \tag{8}$$

Our similarity criteria agree with the results of similarity analysis in [8]. It was required to refine the Weber criterion, which is presented in [8] in the form

$$\pi_4 = \sigma/(\gamma h^2), \tag{9}$$

since it has dimensionality $[m/s^2]$. We proposed dimensionless criterion $\pi_4 = \sigma h/(\nu^2\gamma)$.

Table 2. Similarity analysis

Parameter	Nature	Model
Electrolyte	50 mol % KF–50% AlF_3	20% H_2SO_4
Temperature, °C	700	50
Electrolyte density, kg/m^3	2114	1120
Kinematic electrolyte viscosity, m^2/s	1.28×10^{-6}	7.41×10^{-7}
Dynamic electrolyte viscosity, Pa s	0.00271	0.00083
Surface tension, N/m	0.138	0.0746
Specific gas evolution rate, m^3/(m^2 s)	0.0001	0.0002
Anodic current density, A/cm^2	0.073	0.25
Electrode height, m	0.15	0.075
Anode–cathode distance, m	0.02	0.010
	Similarity criteria	
Bukhbinder criterion	16.24	16.24
Galilean criterion	2×10^{10}	1.2×10^{10}
Weber criterion	5.96×10^6	9.8×10^6
Geometric simplex	7.5	7.5
Non-Newtonian simplex	0.3	0.3
Sedimentation simplex	0.47	0.83

Comparing similarity criteria, we can conclude the similarity of the high-temperature cell and a model (the cell using the electrolysis of the 20% sulfuric acid solution). The results of the numerical calculation are presented in Table 2. The authors additionally introduced the non-Newtonian simplex, which characterizes the ratio of the volume of the solid phase to the total slurry volume, and the sedimentation simplex, which reflects the density ratio of the liquid and the solid phase.

It follows from Table 2 that the data found for the model can be extrapolated to the phenomenon under study with sufficient reliability.

RESULTS OF WATER SIMULATION

Using the results of similarity analysis, we designed an electrochemical cell in which water was decomposed in a slurry consisting of alumina and 20% sulfuric acid solution. The alumina content in the slurry was specified to be 30 vol %. Cell walls were made of 1-mm-thick organic glass. The behavior of oxygen bubbles forming due to the reaction

$$2OH^- - 4e \rightarrow O_2 + 2H^+ \qquad (10)$$

on the anode surface after the formation of the excess oxygen layer was recorded using a Nikon D3100 video camera with the recording frequency of 30 frames/s. The data on the dynamics of bubble motion and growth are acquired.

According to reaction (10), water electrolysis in the acidic medium is accompanied by an increase in acidity of the near-anode layer, which in turn affects the anode potential and, consequently, wettability of the electrode surface with the electrolyte. Thus, acidity of the near-anode layer somewhat affects the bubble shape and, consequently, the flow character of bubbles; however, this influence is small and does not require the refinement of similarity criteria allowing for the approximate character of simulation.

The dynamics of varying the length of four bubbles sequentially coalescing into one bubble is presented in Fig. 1.

The observation for the bubble growth was performed at the current density of 0.05 A/cm^2 in the lower anode part (0–20 mm). An increase in the bubble volume depending on time was most clearly distinguishable by an increase in their length (Fig. 1). The bubble volume increment is attained by gas absorption from the electrolyte, but mainly by coalescence. The presence of the slurry, which hampers bubble lifting, leads to intense coalescence so that the bubble flow regime in the near-anode layer becomes close to the

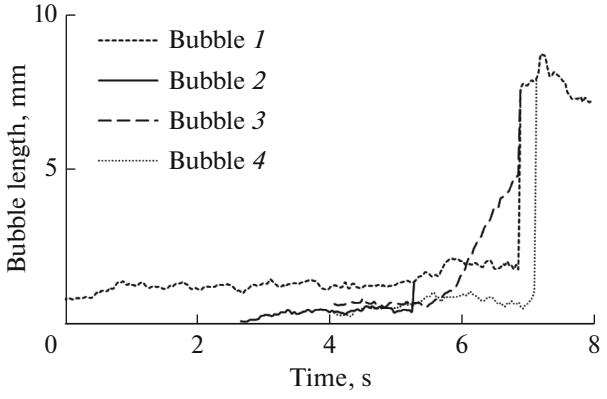

Fig. 1. Subsequent coalescence of bubbles *1–4*.

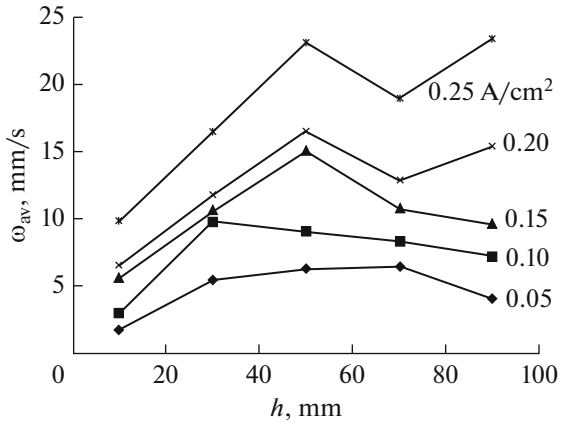

Fig. 2. Dependence of bubble lifting velocity on current density (digits near curves, A/cm^2) at various height marks.

slug regime [14]. The thickness of the electrolyte–gas–slurry three-phase layer (the bubble layer) is ~5 mm. This fact allows us to assume that the electrolysis is possible at l ~ 10 mm.

We determined the average lifting velocity (ω_{av}) of 125 bubbles at various current densities and at various heights. The results are presented in Fig. 2.

The magnitude of ω_{av} depends on height. The bubble lifting rate is largely affected by coalescence and the presence of alumina slurry. The maximum of ω_{av} is observed at the electrode height of 50 mm. After this, the velocity starts to decrease, since the bubbles approach the zone of increased hydrodynamic resistance—the horizontal slurry layer with the bubbles. This layer is characterized by an increased bubble content compared with the initial slurry. The bubbles of larger sizes that are formed at higher current densities (0.2 and 0.25 A/cm^2) pass the electrolyte–air bound-

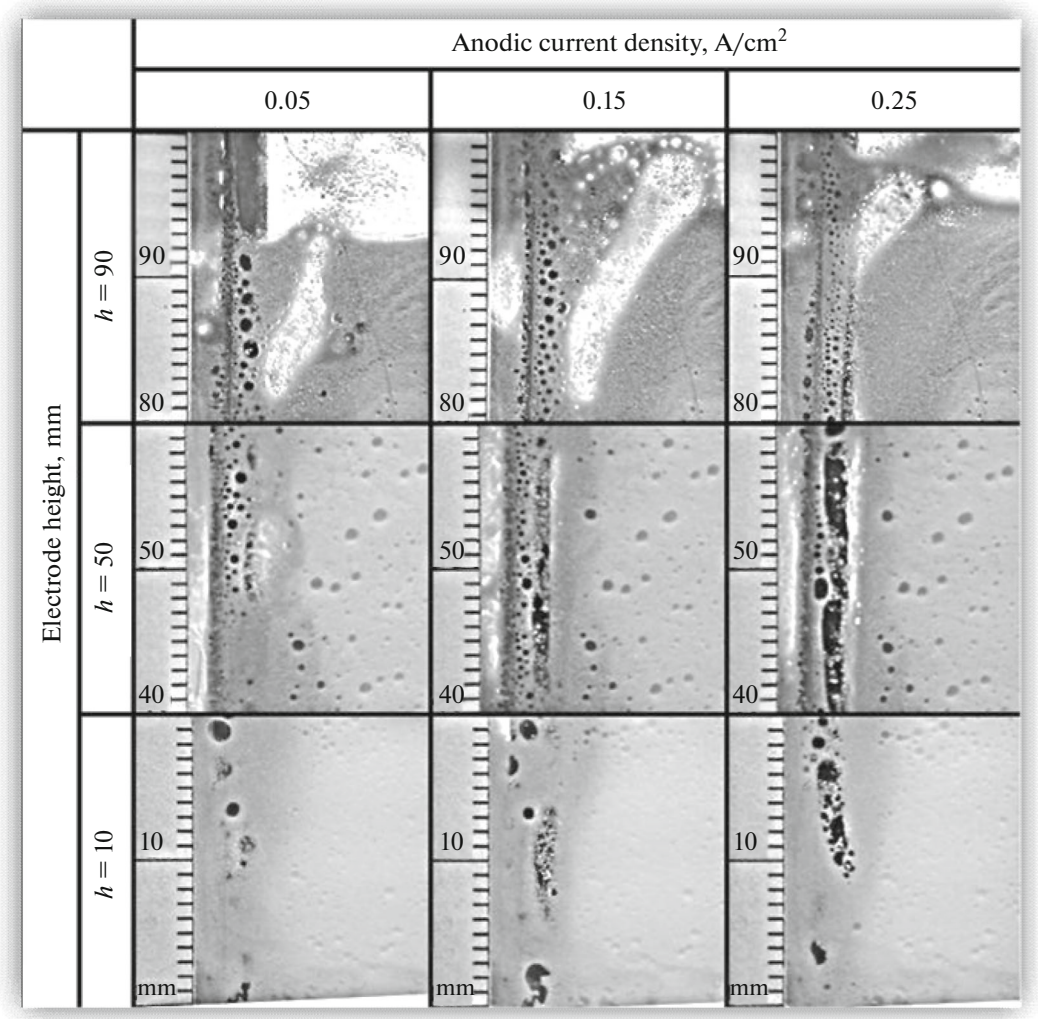

Fig. 3. Appearance of bubbles for various heights at various current densities.

ary more easily, which affects their lifting velocity in upper electrode parts (80–100 mm).

Values of ω_{av} measured by the authors of [15] in various melts were 20–35 cm/s for bubbles 1–2 mm in diameter. In the case of constraint of the bubble layer, the lifting velocity of the bubbles, the width of which reached from 0.8 to 2.3 mm, was from 1 to 2.3 cm/s. Figure 3 shows the bubbles at various current densities.

All images were recorded ~30 s after the beginning of electrolysis. When approaching the electrolyte–air boundary, the bubbles form a peculiar gas "channel," which is clearly seen at higher current densities (0.15 and 0.25 A/cm^2). Lifting bubbles coalesce with this "channel." We can also observe a horizontal slurry layer with the bubbles at the electrolyte–air boundary. The bubbles, when passing through this layer, are subjected to increased resistance and deviate from the initial vertical direction.

CONCLUSIONS

The bubble motion is performed in the slug regime at their lifting velocity of 1.0–2.3 cm/s. The bubble layer thickness is ~5 mm. Evacuation of anode gas from such a dense slurry in free convection conditions is rather efficient and does not lead to the drastically high gas-filling of the near-anode layer. Further investigations will be directed to finding new data on the bubble behavior upon varying the solid phase content, current density, electrode slope, and various granulometric compositions.

REFERENCES

1. Kirpichev, M.V., *Teoriya podobiya* (Similarity Theory), Moscow: Akad. Nauk SSSR, 1953.
2. Huntley, H.E., *Analiz razmernostei* (Dimensional Analysis), Moscow: Mir, 1970.
3. Simakov, D.A., Development of Foundations of Aluminum Electrowinning Technology from Alumina Slurry in Fluoride Melts in Order to Increase Technical and Environmental Characteristics of the Hall–Heroult Process, *Cand. Sci. (Eng.) Dissertation*, Krasnoyarsk: Gos. Univ. Tsvet. Met. i Zolota, 2006.
4. Polyakov, P.V. and Simakov, D.A., RF Patent 2274680, 2006.
5. Polyakov, P.V. and Simakov, D.A., RF Patent 2275443, 2006.
6. Vogt, H., Gas-evolving electrode, in: *Comprehensive treatise of electrochemistry,* New-York–London: Plenum, 1983, vol. 6, pp. 445–489.
7. Sides, P.J., Phenomena and effects of electrolytic gas evolution, in: Modern aspects of electrochemistry, New-York–London: Plenum, 1986, no. 18, pp. 303–355.
8. Ukshe, E.A., Polyakova, G.V., and Medvetskaya, G.A., Chlorine and magnesium dynamics during molten chloride electrolysis, *Zh. Prikl. Khim.*, 1960, no. 10, pp. 2279–2284.
9. Alam, M., Morsi, Y., Yang, W., Mohanarangam, K., Brooks, G., and Chen, J., *Investigation of electrolytic bubble behavior in aluminum smelting cell*, Light Metals, 2013, pp. 591–596.
10. Cassayare, L., Utigart, T.A., and Bouvet, S., Visualizing gas evolution on graphite and oxygen-evolving anodes, *JOM*, 2002, May, pp. 41–45.
11. Das, S., Weerasiri, L.D., and Jegatheeesan, V., *Bubble flow in static magnetic field*, *Light Met.*, 2015, pp. 789–793.
12. Simonsen, A.J., Einasrud, K.E., and Eick, I., The impact of bubble–bubble interaction on anodic gas release: a water model analysis, *Light Met.*, 2015, pp. 795–800.
13. Perron, A., Kiss, L.I., and poncsak, S., Regimes of the movement of bubbles under the anode in an aluminum electrolysis cell, *Light Met.*, 2005, pp. 565–570.
14. Kutepov, A.M., Polyanin, A.D., Zapryanov, Z.D., Vyaz'min, A.V., and Kazenin, D.A. *Khimicheskaya gidrodinamika* (Chemical Hydrodynamics), Moscow: Kvantum, 1996.
15. Shestakov, V.M., Polyakov, P.V., and Burnakin, V.V., Lifting velocity of single bubbles in molten salts, *Teor. Osn. Khim. Tekhnol.*, 1984, vol. 18, no. 3, pp. 118–126.

Translated by N. Korovin